



SAKARYA ÜNİVERSİTESİ

FEN BİLİMLERİ ENSTİTÜSÜ DERGİSİ

Sakarya University Journal of Science
SAUJS

e-ISSN: 2147-835X | Founded: 1997 | Period: Bimonthly | Publisher: Sakarya University
<http://www.saujs.sakarya.edu.tr/en/>

Title: Comparison of Maximum Power Point Tracking Methods Using Metaheuristic Optimization Algorithms for Photovoltaic Systems

Authors: Necati BİLGİN, İrfan YAZICI

Received: 2021-05-11 18:11:39

Accepted: 2021-07-14 15:46:41

Article Type: Research Article

Volume: 25

Issue: 4

Month: August

Year: 2021

Pages: 1075-1085

How to cite

Necati BİLGİN, İrfan YAZICI; (2021), Comparison of Maximum Power Point Tracking Methods Using Metaheuristic Optimization Algorithms for Photovoltaic Systems.

Sakarya University Journal of Science, 25(4), 1075-1085, DOI:

<https://doi.org/10.16984/saufenbilder.936254>

Access link

<http://www.saujs.sakarya.edu.tr/en/pub/issue/64755/936254>

New submission to SAUJS

<http://dergipark.org.tr/en/journal/1115/submission/step/manuscript/new>

perturb and observe [7]. Miyatake M. et al. compared the results obtained from particle swarm optimization with Fibonacci search method, hill climb method and constant voltage methods [8]. Eltamaly A.M. et al. proposed a new method for maximum power point tracking (MPPT) based on the bat optimization [9]. Ding J. et al. proposed a new MPPT method created by combining particle swarm optimization and cuckoo search optimization [10]. Dhivya P. et al. compared the MPPT results obtained by perturb and observe method, particle swarm optimization and firefly optimization [11].

In this study, a simulation study has been carried out with a PV system consisting of a PV array, boost converter and MPPT controller. In order to see the performance of different optimization methods on MPPT, 4 different metaheuristic optimization techniques has been used and the PV system output powers obtained as a result of the simulation has been compared.

2. PHOTOVOLTAIC SYSTEM

PV systems convert the energy in sunlight directly into electrical energy. This transformation was first discovered by French scientist Alexandre Edmond Becquerel in 1839 [12]. Later, it was used in space research with the discovery of semiconductor materials such as silicon with PV property. Although it was not preferred in the past due to its application cost, its use has gained great momentum in the last 20 years.

The main applications of PV systems are stand-alone (water pumping, home and street lighting, electric vehicles, military and space applications) or grid-dependent configurations (hybrid systems, power plants) whose use has increased recently [13].

Basic elements of PV systems are cells formed with semiconductor diodes. Cells can be made of various semiconductor materials. When the cell absorbs photons from sunlight, electrons are freed from silicon atoms and are attracted by a grid of metal conductors, resulting in a direct current flow and electricity is produced [14].

One-diode or two-diode equivalent circuits are used to model the cell. In this study, the single diode circuit model given in Figure 1 is used.

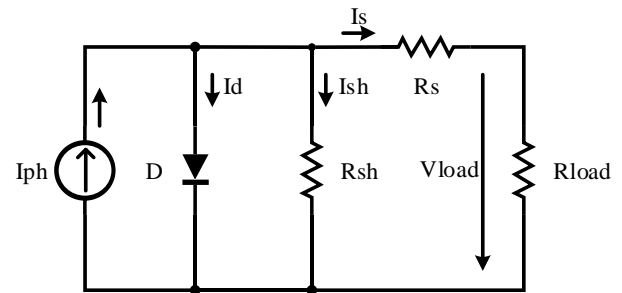


Figure 1 One-diode equivalent circuit

For one-diode model, the output current is obtained with Kirchoff's current law given in equation (1) [15].

$$I_s = I_{ph} - I_d - I_{sh} \quad (1)$$

Here, I_{ph} is the photocurrent generated, I_d is the saturation current, I_{sh} represents the current flowing through the parallel resistor. Mathematical expression of the cell given in equation (2) is obtained when the saturation current and the current flowing through the parallel resistance are reformed in the equation [15].

$$I_s = I_{ph} - I_0 \left\{ \exp \left[\frac{q(V + R_s I_s)}{nkT_k} \right] - 1 \right\} - \frac{V + R_s I_s}{R_{sh}} \quad (2)$$

Here, I_0 is the diode saturation current, I_s and V are the current and voltage of the PV cell, respectively, and R_{sh} and R_s are the parallel and series resistors, respectively. k represents Boltzmann constant with value $1.38 \times 10^{-23} J/K$, q charge amount of an electron with value $1.602 \times 10^{-19} C$, and T_k is cell temperature.

The cellular groups formed in the protective laminated surface are called modules in order to reduce the effects of cells from various environmental conditions and to obtain higher powers compared to cells. Cells are connected in parallel to increase the current and in series to increase the voltage, depending on the area of use.

The groups of modules obtained by connecting modules in series or in parallel in order to obtain higher powers compared to modules are called arrays. When constituting arrays, modules are connected in parallel to increase the current and in series to increase the voltage.

In PV systems, the output power varies depending on solar irradiation and temperature. As the solar irradiation increases, the current increases and so the output power also increases. On the other hand, as the temperature increases, the voltage decreases and so the output power decreases. Changes in current, voltage and output power according to solar irradiation and temperature are given in Figure 2 and Figure 3.

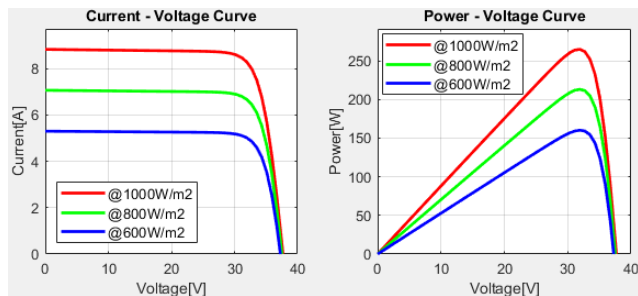


Figure 2 Effects of solar irradiation on I-V and P-V curves

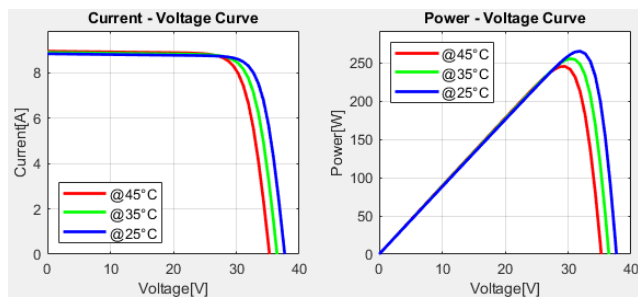


Figure 3 Effects of temperature on I-V and P-V curves

In a system built with PV arrays, some modules may generate less power than others due to partial shading caused by environmental causes such as buildings, trees, and clouds [16]. In such cases, the efficiency of the system decreases and less output power is obtained. In Figure 4, the power-voltage (P-V) curves of the changes in the output power of an array whose modules are subject to partial shading are given. As can be seen from the curves, when the modules on the system are exposed to equal sunlight, only one maximum

power point (MPP) is formed in the P-V curve and this point is the global MPP. However, when the modules are exposed to different sunlight, more than one MPP is formed, the largest of these points is the global MPP and the others are the local MPP.

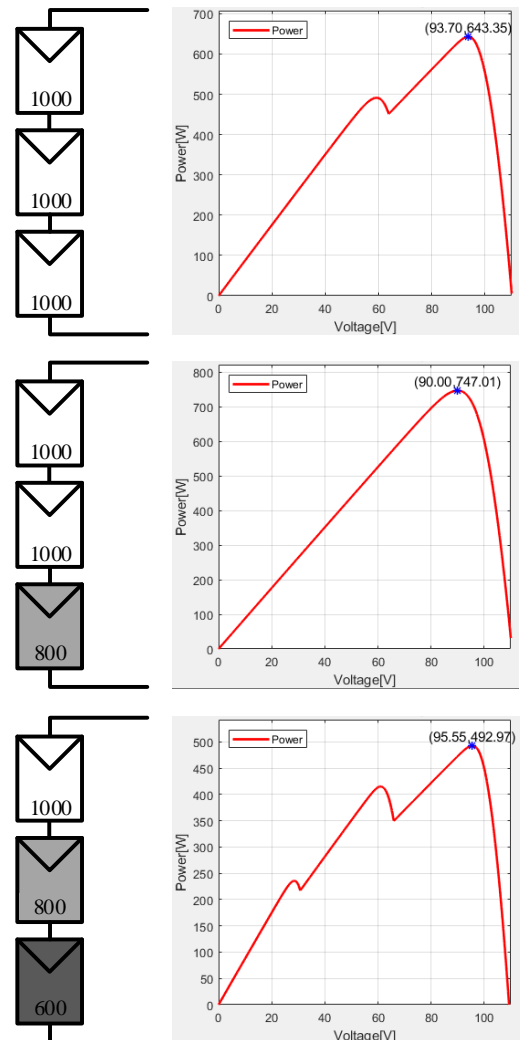


Figure 4 Effects of partially shaded condition on P-V curve

In this study, boost type DC-DC converter is used to adjust the power value drawn from the PV system. In Figure 5, MPPT block diagram consisting of PV system, MPPT controller and boost converter is given.

In the boost converter, when the S switch is ON, the D diode is reverse polarized, the V_{PV} input voltage is applied to the L inductor. The current increases from zero current in the inductor when operating in discontinuous mode or from a certain

starting current when operating in continuous mode to its peak value.

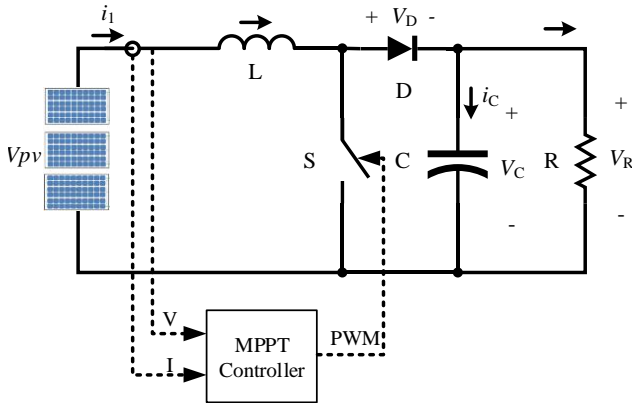


Figure 5 MPPT block diagram

When the S switch is turned OFF, the voltage on the inductor is reversed, causing the diode voltage to be above the input voltage. The diode V_{PV} transfers the energy of the inductor L to these elements, as well as the energy transferred to the capacitor C and the load R by the input voltage. In this way, V_R voltage is greater than V_{PV} voltage. In this study, equations (3), (4) and (5) has been used while calculating the boost converter parameters [17].

$$V_0 = \frac{V_{in}}{1-D} \quad (3)$$

$$L_{\min} = \frac{R(1-D)^2 D}{2f_s} \quad (4)$$

$$C_{\min} = \frac{DV_0}{\Delta V_0 f_s R} \quad (5)$$

Here, V_0 is the output voltage of the converter, V_{in} is the PV array voltage, and D is the duty ratio of the PWM sign that determines the ON-OFF position of the switching element in the circuit. R is the load resistance, f_s is the sampling frequency, and ΔV_0 represents the ripple in the output voltage.

3. OPTIMIZATION ALGORITHMS

3.1. Particle Swarm Optimization (PSO)

PSO, developed by James Kennedy and Russell C. Eberhart in 1995, is an optimization algorithm based on socio-psychological theory [18]. The algorithm deals with the search for optimum values of individuals called particles in a population.

In each iteration performed in the PSO algorithm, the positions and velocities of each particle and the global optimum position are updated. The following equations (6) and (7) are used to update the position and velocity of the particles in the population [19].

$$v_i(k+1) = \omega \times v_i(k) + c_1 \times r_1 \times (P_{best_i} - x_i(k)) \quad (6)$$

$$+ c_2 \times r_2 \times (G_{best} - x_i(k))$$

$$x_i(k+1) = x_i(k) + v_i(k+1) \quad (7)$$

Here, $v_i(k)$ is velocity for the i 'th particle at the k 'th iteration, ω is the weight function constant, c_1 and c_2 positive constants in the range of [0, 2], r_1 and r_2 uniformly distributed random numbers in the range of [0, 1]. $x_i(k)$ is position for the i 'th particle at the k 'th iteration, P_{best_i} is the best position for the i 'th particle and G_{best} represents the best position so far. The flowchart used for MPPT based on PSO is given in Figure 6 [20].

3.2. Cuckoo Search Optimization (CSO)

CSO was developed by Xin-She Yang and Suash Deb in 2009 by transforming the parasitic life situation resulting from some cuckoo birds laying their eggs in their nests to other birds' nests into an optimization technique [21]. Some cuckoo species can mimic the shape and color of the nesting bird, which increases the likelihood of breeding. It is also known that cuckoo birds lay their eggs at a certain time, so that their eggs hatch some time before that of the nest-owning bird. After early hatching, cuckoo birds destroy the eggs of some nesting birds to increase their chicks' chances of getting more food. It is also

possible that nesting birds will notice the cuckoo's eggs and destroy them. Sometimes nesting birds leave their nest altogether and go elsewhere to build a new nest [22]. New nests in CSO are obtained by using the Lévy flight with the following equation (8) [23].

Here, $x_{ij}(k)$ is the nest, $\alpha = a_0(x_{best} - x_i)$ and α_0 is the initial step interval, \oplus and λ represents the entry-wise multiplication operation and the flight parameter of Lévy, respectively. The Lévy flight is a random walk in which the step lengths have a Lévy distribution, which is a probability distribution. The flow diagram used for MPPT based on CSO is given in Figure 7 [24].

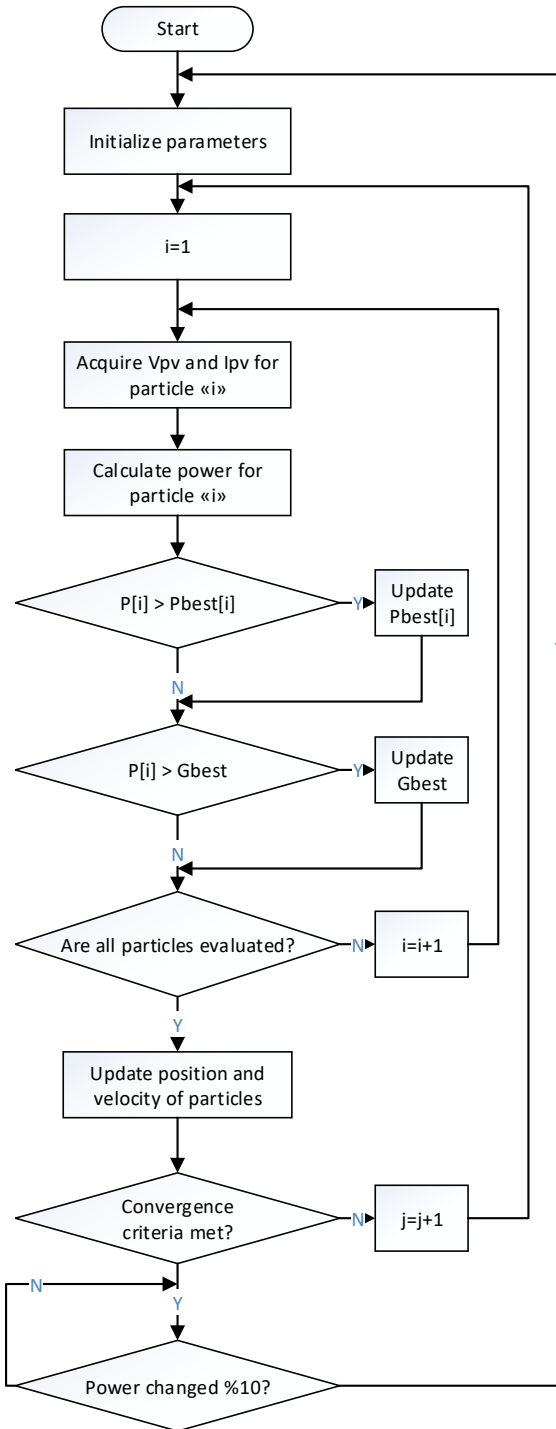


Figure 6 Flowchart of PSO algorithm

$$x_{ij}(k+1) = x_{ij}(k) + \alpha \oplus Levy(\lambda) \quad (8)$$

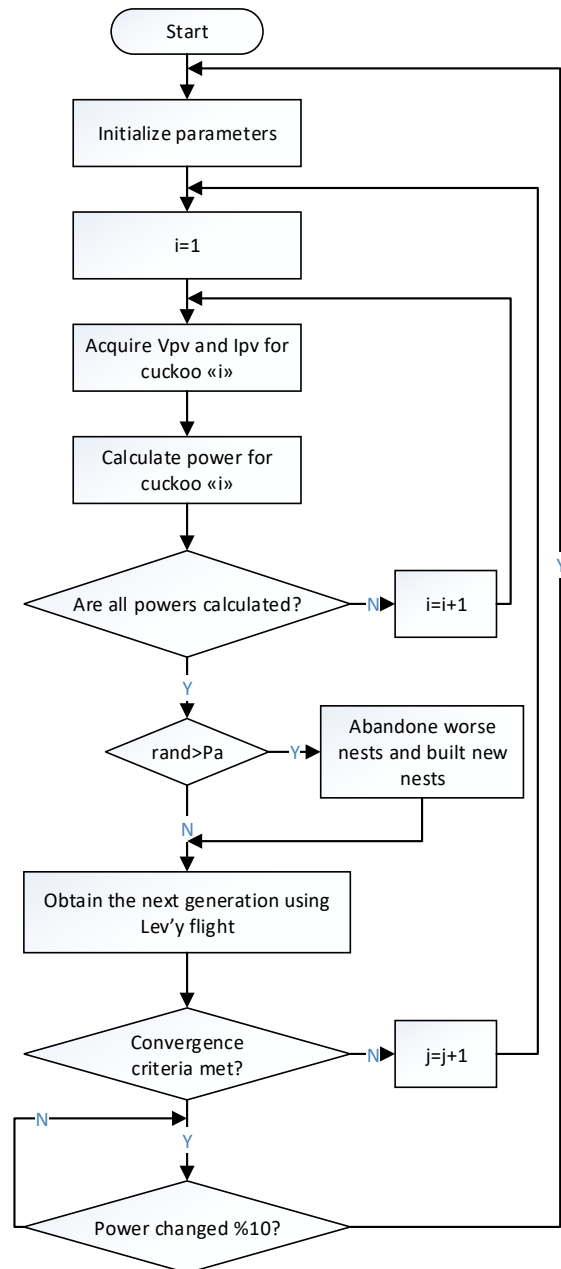


Figure 7 Flowchart of CSO algorithm

3.3. Bat Optimization (BAO)

BAO is one of the algorithms developed by taking inspiration from nature. The algorithm developed by Xin-She Yang in 2010 is based on sound echolocation of bats. Bats express their distance to prey or food by changing the frequencies of the sounds they make. In this way, it enables the population to obtain more solutions that are diverse.

For the bat algorithm, the following equations (9), (10) and (11) are basically used [25].

$$f_i = f_{\min} + \beta(f_{\max} - f_{\min}) \quad (9)$$

$$v_i^k = v_i^{k-1} + (x_i^{k-1} - x_{best})f_i \quad (10)$$

$$x_i^k = x_i^{k-1} + v_i^k \quad (11)$$

Here, $\beta \in [0,1]$ is a random number, x_{best} is the best position in bats, f_i is the frequency for i 'th bat, f_{\min} and f_{\max} are the minimum and maximum frequency, respectively. Each bat initially has a randomly assigned frequency between f_{\min} and f_{\max} . x_i^k and v_i^k represent the position and velocity of the i 'th bat at the k 'th iteration, respectively. The flowchart of the BAO algorithm is given in Figure 8 [18].

3.4. Firefly Optimization (FFO)

FFO is a meta-heuristic optimization technique based on swarm intelligence and inspired by the light emitted by fireflies, developed by Xin-She Yang in 2008 [26]. The two main functions of the light emitted by fireflies are to attract mating partners and potential prey.

The positions of fireflies in FFO are updated by equation (12) [27].

$$x_i^{k+1} = x_i^k + \beta(r) \times (x_i^k - x_j^k) + \alpha(rand - \frac{1}{2}) \quad (12)$$

Here, x_i^k and x_j^k are the position of i and j fireflies at the k 'th iteration, respectively, $\beta(r)$

is the attraction function. Flowchart of FFO algorithm is given in Figure 9 [28].

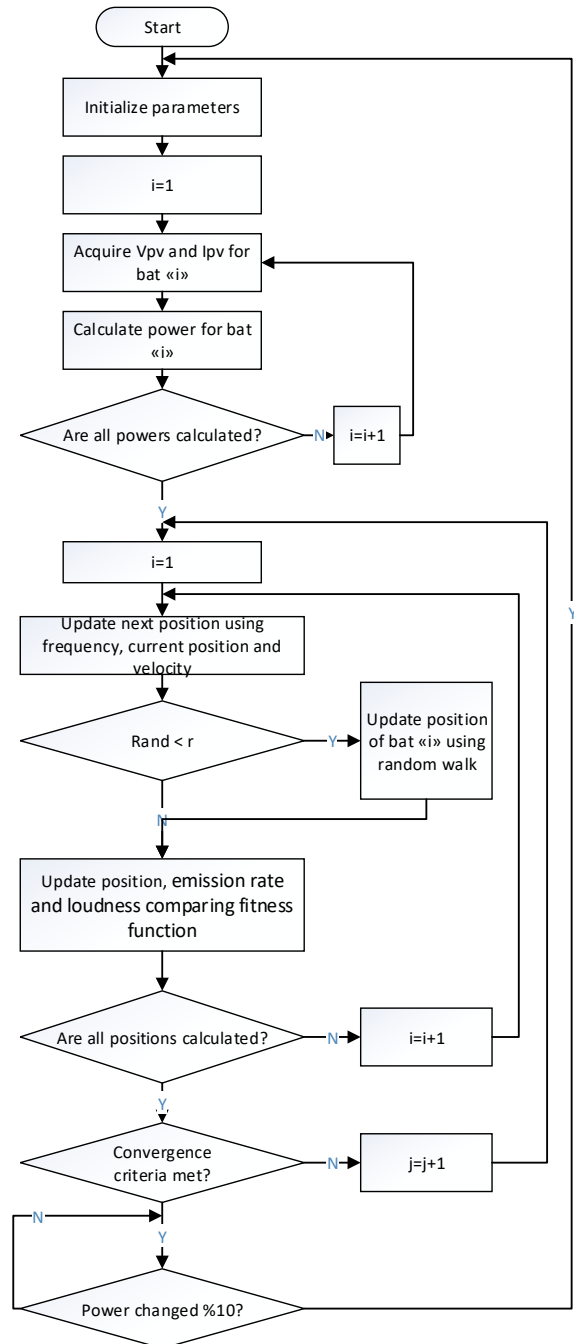


Figure 8 Flowchart of BAO algorithm

4. SIMULATION RESULTS

In order to compare the MPPT performance of the optimization algorithms given above, the system consisting of 3-PV modules connected in series has been examined for two scenarios involving partial shading. The simulation study has been

carried out with Matlab R2020b software. For the scenarios, the simulation time of 1.5 s is divided into 3 equal parts and a different partial shading conditions are discussed at every 0.5 s. Partially shaded conditions and scenarios created are given in Table 1 and Table 2.

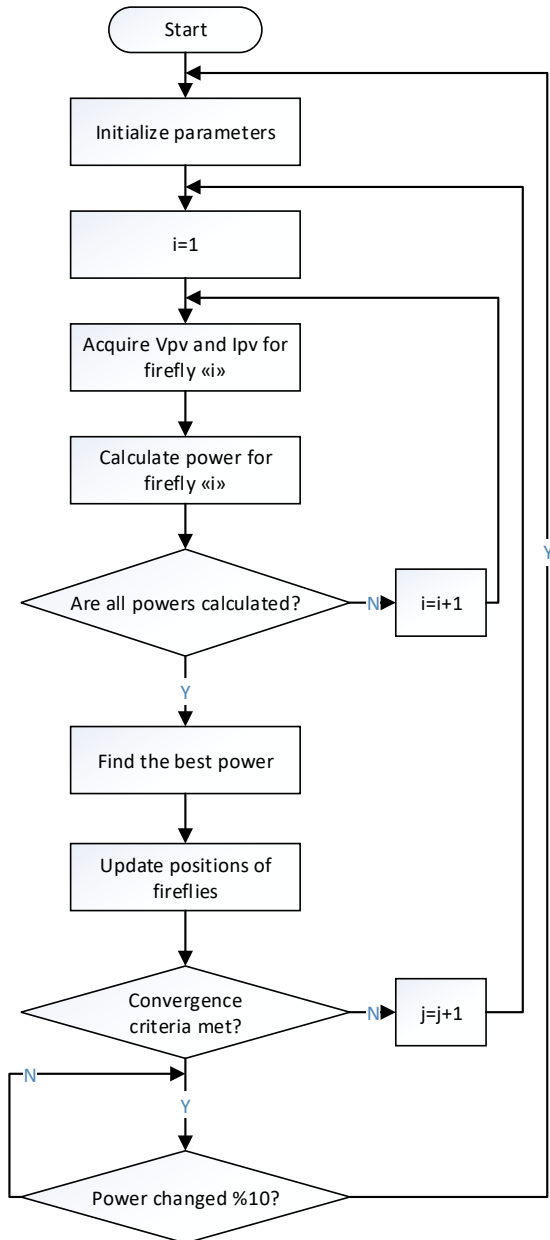


Figure 9 Flowchart of FFO algorithm

The system has constraint for maximum power at operating conditions due to nonlinear and inverse proportional relation between voltage and current as seen in Figure 2 and Figure 3. While the current varies 0 to short circuit current (I_{sc}), the voltage varies 0 to open circuit voltage (V_{oc}). When

controlled current or voltage, the system can be operated at maximum power. In this study, voltage control mode has been selected and DC-DC boost converter has been used in order to control voltage. Voltage has been controlled by changing of the duty ratio of converter under limits of 0 to 1.

Table 1 Partially shaded conditions (PSC)

PSC	Module 1	Module 2	Module 3	Maximum Power(P_{max})
PSC-1	1000	1000	1000	747
PSC-2	760	888	401	391.4
PSC-3	994	977	598	496
PSC-4	943	426	984	472.1
PSC-5	553	278	436	229.4
PSC-6	329	864	540	286.4

Table 2 Simulated scenerios

Scenario	0 to 0.5 s	0.5 to 1.0 s	1.0 to 1.5 s
Scenario-1	PSC-1	PSC-5	PSC-3
Scenario-2	PSC-2	PSC-6	PSC-4

4.1. Power obtained from Scenario-1

In Scenario-1, all of the algorithms have reached MPP as seen in Figure 10. However, the times of algorithms to reach the global MPP has different, and the algorithm with the best value in terms of time has been FFO. In order to see the changes in the output power in more detail, the power between 0.5 and 0.8 s is shown in Figure 11 in a zoomed way. The MPP values reached by the algorithms are given in Table 3. According to Figure 10, Figure 11 and Table 3, even if FFO has the highest P_{avg} , PSO, CSO and BAO algorithms have the lowest power deviation at the MPP. As a result, if simulation period was be longer, PSO, CSO and BAO would obtain higher power depending on the PSC.

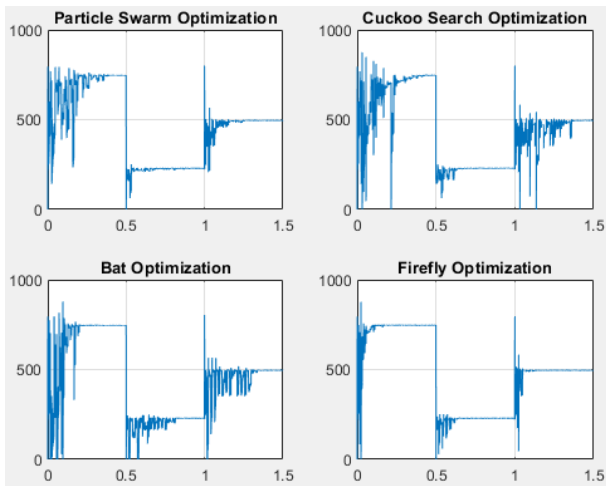


Figure 10 PV system output power for Scenario-1

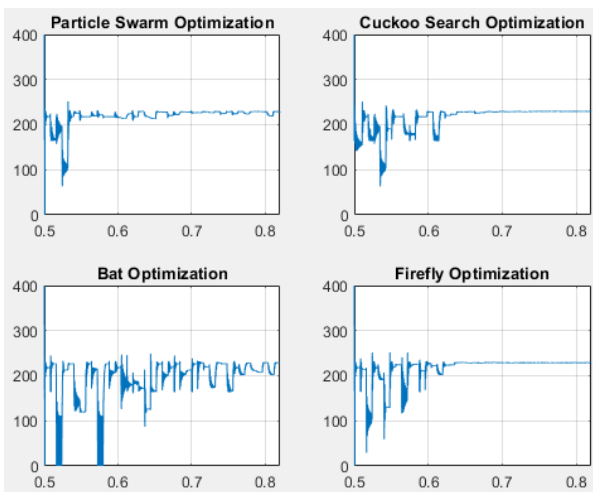


Figure 11 PV system output power between 0.5 and 0.8 s for Scenario-1

Table 3

Power values obtained with Scenario-1

Algorithm	$P_{\max1}$ (PSC-1)	$P_{\max2}$ (PSC-5)	$P_{\max3}$ (PSC-3)	P_{avg}
Theoric	747.00	229.4	496.00	-
PSO	746.78	228.58	495.93	500.99
CSO	744.16	229.43	496.05	482.09
BAO	746.07	229.05	496.08	491.47
FFO	746.77	229.03	495.93	531.46

4.2. Power obtained from Scenario-2

In Scenario-2, all of the algorithms have reached MPP as seen in Figure 12. However, since the individuals used in CSO cannot converge to each other, they create oscillations in the output power. In addition, the times of algorithms to reach the global MPP has differed, and the algorithm with the best value in terms of time has been ABO. The

MPP values reached by the algorithms are given in Table 4. As shown in Figure 12 and Table 4, even if FFO has the highest P_{avg} , difference between theoretic power and power obtained by algorithm has been lowest for PSO at each MPP. As a result, if the simulation period was longer, best algorithm would be PSO for scenario-2.

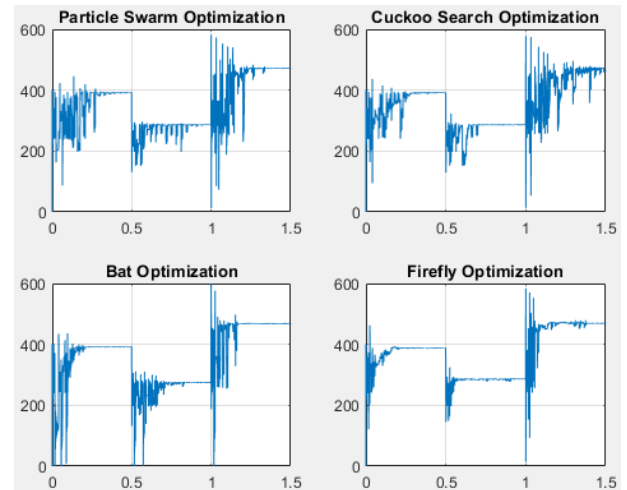


Figure 12 PV system output power for Scenario-2

Table 4 Power values obtained with Scenario-2

Algorithm	$P_{\max1}$ (PSC-2)	$P_{\max2}$ (PSC-6)	$P_{\max3}$ (PSC-4)	P_{avg}
Theoric	391.4	286.4	472.1	-
PSO	391.22	286.40	471.63	362.19
CSO	391.18	286.26	467.57	364.35
BAO	391.18	275.05	468.28	365.21
FFO	387.64	286.23	468.96	377.63

5. CONCLUSION

In this study, 4 different optimization techniques as MPPT method in PV systems have been examined comparatively in case of partial shading conditions. Among the optimization algorithms examined in the simulation studies, it has been shown that the FFO method provides better results in terms of the reaching time to the maximum power and value of the maximum power.

Funding

The author (s) has no received any financial support for the research, authorship or publication of this study.

The Declaration of Conflict of Interest/ Common Interest

The authors have declared no conflict of interest or common interest.

Authors' Contribution

N.B.: Literature review, writing codes of simulation, carrying out the simulation studies and writing the article

İ.Y.: Determining the method and scope of research and coordinating its writing

The Declaration of Ethics Committee Approval

This study does not require ethics committee permission or any special permission.

The Declaration of Research and Publication Ethics

The authors of the paper declare that they comply with the scientific, ethical and quotation rules of SAUJS in all processes of the paper and that they do not make any falsification on the data collected. In addition, they declare that Sakarya University Journal of Science and its editorial board have no responsibility for any ethical violations that may be encountered, and that this study has not been evaluated in any academic publication environment other than Sakarya University Journal of Science.

REFERENCES

- [1] K. K. Tse, M. T. Ho, H. S. -H. Chung, and S. Y. Hui, "A novel maximum power point tracker for PV panels using switching frequency modulation," *IEEE Transactions on Power Electronics*, vol. 17, no. 6, pp. 980-989, 2002.
- [2] O. Ezinwanne, F. Zhongwen, and L. Zhijun, "Energy performance and cost comparison of MPPT techniques for photovoltaics and other applications," *Energy Procedia*, vol. 107, pp. 297-303, 2017.
- [3] S. E. Babaa, M. Armstrong, V. Pickert, "Overview of maximum power point tracking control methods for PV systems," *Journal of Power and Energy Engineering*, vol. 2, no. 8, pp. 59-72, 2014.
- [4] F. D. Murdianto, M. Z. Efendi, R. E. Setiawan, and A. S. L. Hermawan, "Comparison method of MPSO, FPA, and GWO algorithm in MPPT SEPIC converter under dynamic partial shading condition," 2017 International Conference on Advanced Mechatronics, Intelligent Manufacture, and Industrial Automation (ICAMIMIA), Surabaya, pp. 315-320, 2017.
- [5] N. Khanam, B. H. Khan, and T. Imtiaz, "Maximum power extraction of solar PV system using meta-heuristic MPPT techniques: A comparative study," 2019 International Conference on Electrical, Electronics and Computer Engineering (UPCON), Aligarh, pp. 1-6, 2019.
- [6] M. A. Dirmawan, Suhariningsih, and R. Rakhmawati, "The comparison performance of MPPT perturb and observe, fuzzy logic controller, and flower pollination algorithm in normal and partial shading condition," 2020 International Electronics Symposium (IES), Surabaya, pp. 7-13, 2020.
- [7] A. Dolara, R. Faranda, S. Leva, "Energy comparison of seven MPPT techniques for PV systems," *Journal of Electromagnetic Analysis and Applications*, vol. 1, no. 3, pp. 152-162, 2009.
- [8] M. Miyatake, M. Veerachary, F. Toriumi, N. Fujii, and H. Ko, "Maximum power point tracking of multiple photovoltaic arrays: A PSO approach," *IEEE Transactions on Aerospace and Electronic Systems*, vol. 47, no. 1, pp. 367-380, 2011.
- [9] A. M. Eltamaly, M. S. Al-Saud, and A. G. Abokhalil, "A novel bat algorithm strategy for maximum power point tracker of

- photovoltaic energy systems under dynamic partial shading,” *IEEE Access*, vol. 8, pp. 10048-10060, 2020.
- [10] J. Ding, Q. Wang, Q. Zhang, Q. Ye, and Y. Ma, “A hybrid particle swarm optimization-cuckoo search algorithm and its engineering applications,” *Mathematical Problems in Engineering*, vol. 2019, pp. 1-12, 2019.
- [11] P. Dhivya, and K. R. Kumar, “MPPT based control of sepic converter using firefly algorithm for solar PV system under partial shaded conditions,” *2017 International Conference on Innovations in Green Energy and Healthcare Technologies (IGEHT)*, Coimbatore, pp. 1-8, 2017.
- [12] W. Xiao, “Photovoltaic power system modeling, design, and control,” Chennai, Wiley, 2017.
- [13] R. Faranda, and S. Leva, “Energy comparison of MPPT techniques for PV Systems,” *WSEAS Transactions on Power Systems*, vol. 3, no. 6, pp. 446-455, 2008.
- [14] M. R. Shaikh, S. Shaikh, S. Waghmare, S. Labade, and A. Tekale, “A review paper on electricity generation from solar energy,” *International Journal for Research in Applied Science and Engineering Technology*, vol. 5, no. 9, pp. 1884-1889, 2017.
- [15] R. Anand, S. D, and B. Kumar, “Global maximum power point tracking for PV array under partial shading using cuckoo search,” *2020 IEEE 9th Power India International Conference (PIICON)*, Sonapat, pp. 1-6, 2020.
- [16] R.-E. Precup, T. Kamal, and S. Z. Hassan, “Solar photovoltaic power plants - Advanced control and optimization techniques,” Singapore, Springer, 2019.
- [17] K. Aygül, “Butterfly optimization algorithm based maximum power point tracking of photovoltaic systems under partial shading condition,” Adana, Cukurova University, 2019.
- [18] M. V. Rocha, L. P. Sampaio, and S. A. Silva, “Comparative analysis of ABC, Bat, GWO and PSO algorithms for MPPT in PV systems,” *8th International Conference on Renewable Energy Research and Applications*, Brasov, pp. 347-352, 2019.
- [19] G. Dilep, and S. Singh, “An improved particle swarm optimization based maximum power point tracking algorithm for PV system operating under partial shading conditions,” *Solar Energy*, vol. 158, pp. 1006-1015, 2017.
- [20] H. Chaieb, and A. Sakly, “Review and comparison of BAT and PSO MPPT’s based algorithms for photovoltaic system,” *WSEAS Transactions on Power Systems*, vol. 13, pp. 108-117, 2018.
- [21] A. M. Kamoona, J. C. Patra and A. Stojcevski, “An enhanced cuckoo search algorithm for solving optimization problems,” *2018 IEEE Congress on Evolutionary Computation (CEC)*, Rio de Janeiro, pp. 1-6, 2018.
- [22] J. Ahmed, and Z. Salam, “A soft computing MPPT for PV system based on cuckoo search algorithm,” *4th International Conference on Power Engineering, Energy and Electrical Drives*, Istanbul, pp. 558-562, 2013.
- [23] M. I. Mosaad, M. O. el-Raouf, M. A. Al-Ahmar, and F. A. Banakher, “Maximum power point tracking of PV system based cuckoo search algorithm; review and comparison,” *Energy Procedia*, vol. 162, pp. 117-126, 2019.
- [24] T. P. Dao, “Cuckoo search algorithm: Statistical-based optimization approach and engineering applications,” Singapore, Springer, 2021.

- [25] A. Brabazon, and S. McGarraghy, "Foraging-inspired optimisation algorithms," Dublin, Springer, 2018.
- [26] K. Sundareswaran, S. Peddapati, and S. Palani, "MPPT of PV systems under partial shaded conditions through a colony of flashing fireflies," *IEEE Transactions on Energy Conversion*, vol. 29, no. 2, pp. 463-472, 2014.
- [27] M. Mohanty, S. Selvakumar, C. Koodalsamy, and S. Simon, "Global maximum operating point tracking for PV system using fast convergence firefly algorithm," *Turkish Journal of Electrical Engineering & Computer Sciences*, vol. 27, pp. 4640-4658, 2019.
- [28] L. N. Palupi, T. Winarno, A. Pracoyo, and L. Ardhenta, "Adaptive voltage control for MPPT-firefly algorithm output in PV system," *IOP Conference Series: Materials Science and Engineering, East Java*, vol. 732, pp. 1-9, 2020.